



MICROSTRUCTURAL AND TRANSIENT THERMAL ANALYSIS OF TIG WELDED JOINT SAE 2205 WITH AISI 304 WITH AISI 308 FILLER METAL

C.Selva Ganesh¹, Dr.T.Vigraman (M.E., Ph.D)^{*2}, D.Sujith³, M.Velmanikandan⁴, T.Vetrivel⁵

^{1,2} Associate Professor S.G, Department of Mechanical Engineering, National Engineering College, Kovilpatti, Tamil Nadu, India

^{3,4,5} Final Year Students, Department of Mechanical Engineering, National Engineering College, Kovilpatti, Tamil Nadu, India

Abstract:

In the present work SAE 2205 is welded with AISI 304 using AISI 308 filler wire. TIG welding current was maintained at 110, 120 and 130 Amp and the voltage was set at 40 Volt. A constant welding speed of 0.5 mm/s was maintained for all the experiments. The optical microscopic examination of the welded samples revealed the presence of recrystallized zone, mushy zone at the weld metal SAE 2205 side and columnar grains adjacent to the heat affected zone. The maximum hardness value of Rc 29 was observed in the welded region. The increase in hardness value was attributed to absorption of oxygen in the weld metal during welding and solidification of the weld metal. A maximum yield strength of 354 MPa and an ultimate tensile strength value of 549 MPa were obtained for the samples processed at 130 Amp. Combined transient thermal and stress analysis was performed for the dissimilar stainless steel joints made between SAE 2206 and AISI 304L. A maximum Von Mises stress of 85 MPa was obtained for the weld joints made between stainless steel AISI 304 and stainless steel SAE 2205.

Keywords: Duplex Stainless Steel SAE 2205; Dissimilar Weld; Micrograph; Hardness, Tensile Strength; ANSYS; Transient Thermal Analysis.

Cite This Article: C.Selva Ganesh, Dr.T.Vigraman M, D.Sujith, M.Velmanikandan, and T.Vetrivel. (2017). "MICROSTRUCTURAL AND TRANSIENT THERMAL ANALYSIS OF TIG WELDED JOINT SAE 2205 WITH AISI 304 WITH AISI 308 FILLER METAL." *International Journal of Engineering Technologies and Management Research*, 4(10), 15-25. DOI: 10.5281/zenodo.1040736.

1. Introduction

In general stainless steels have any one single phase such as ferrite, austenite and martensite also they have dual phase's ferrite and austenite. Kohyama et.al [1] performed TIG welding of 15 mm thick AISI 316 steel plates and studied the effect of welding parameters such as welding current, voltage and welding speed on microstructure of the weld metal. Juang et al [2] performed TIG welding on stainless steels and studied the effect of weld parameters on weld pool geometry. Duplex stainless steels have both ferrite and austenite structure and their amounts may vary

depending upon composition of the alloy. Duplex stainless steel (DSS) possesses high strength and good corrosion resistance properties. Therefore, duplex stainless steels are used for corrosion resistance applications. DSS cannot be used for high temperature applications because of sigma phase formation at higher temperatures. Austenitic stainless steel grade AISI 304 possess, austenite structure, good strength and high temperature properties, therefore, this stainless steel is used as general purpose alloy. In addition AISI 304 steel possesses good corrosion resistance properties because of this it is used in corrosive environment. The AISI 308 stainless steel is used as filler metal having yield and tensile strengths 350 and 540 MPa, respectively. The filler metal is an austenitic stainless steel contains equal amounts of nickel as AISI 304 base metal. Use of AISI 308 filler metal results in closer control of ferrite phase at the weld region resulting in enhancement of corrosion resistance properties. Furthermore, filler metal AISI 308 increases the joint strength above the base metal AISI 304 stainless steel. TIG welding is suitable for making high strength joints and prevents absorption of interstitial elements during welding.

Raghuvir Singh et al [3] studied the effect of TIG welding parameters on AISI 304L welded joints and observed that depth of penetration was high with SiO₂ flux and welding current. Kang et.al [4] studied the effect of shielding gases in 12 mm thick AISI 304 austenite stainless steel TIG welded joints. Ahmet Durgutlu [5] investigated the effect of hydrogen in varying proportions in argon as a shielding gas on TIG welding of stainless steels and the welded joints exhibited reduced mechanical properties with increased hydrogen content in Argon gas. The dissimilar metal weld joints may fail well below its strength because of residual stresses built in the welded joints. The reason for decrease in strength could be difference in thermal expansion coefficients and thermally induced plastic deformation. Zuheir Barsoum et al [6] performed residual stress analysis and fatigue assessment of welded steel structures to develop simplified procedures for analysis of residual stresses, their relaxation and influence on fatigue life. Janakiram and Venkateswara Rao [7] performed analysis of temperature distribution of different welded joints in shipbuilding. The SOLID87 was well suited to model irregular meshes. Ya Tao Wu et al [8] performed residual stress study at the dissimilar metal butt joint due to the weld overlay repair on a nuclear power plant nozzle using ANSYS. TIG welding is most widely applied for welding reactive elements and for making root pass welds in boiler shells. In the present study DSS SAE 2205 is welded with AISI 304 with AISI 308 steel as filler metal. A superior corrosion resistant material SAE 2205 is joined with an austenitic stainless steel AISI 304 and the mechanical and metallurgical characteristics are studied. Further, the dissimilar joints are performed thermal analysis using ANSYS software to find the temperature distribution and residual stress built in the joint.

2. Experimental Work

The SAE 2205 and AISI 304 alloy in the plate form is cut to the required size of 60 mm × 40 mm × 3 mm. The edges were machined to get a chamfer of 3 mm. the composition of the base metal is presented in Table 1. The filler wire used for TIG welding was AISI 308 steel. In the present study a matching electrode was used for joining the two dissimilar grades of stainless steels. TIG welding of the butt joints was carried out by varying the parameter welding current alone. The current values were set at 110, 120 and 130 Amp. The other two parameters like welding voltage and welding speed were maintained at 35 V and 0.5mm/s for all trials.

The welded samples were machined using Electric Discharge Machining Technique to obtain tensile test specimens of 120 mm × 18 mm × 3 mm and metallography specimens of size 30 mm × 10 mm × 6 mm in sizes. The macrohardness assessment was carried out using a Rockwell hardness testing machine. A test load of 150 Kgf was applied and hardness values were measured on the ‘C’ scale. The tensile test specimen was prepared as per ASTM E8M and is shown in Figure 1 (a). The tensile test was conducted with a computerized tensile testing machine. The metallography specimen was prepared by finishing with various grades of abrasive sheets such as 220, 320, 400, 600, 800, 1000 and 1200 and finally polished with slurry of Al₂O₃ for two minutes. The polished specimens were etched with a mixture of 5ml Hydro Chloric acid (HCl), 2g picric acid and 100 ml ethyl alcohol. The specimens were examined with Olympus inverted type of microscope.

Table 1 Chemical composition of the base metals and the filler metal.

Material	P%	S%	N%	C%	Si%	Mn%	Mo%	Ni%	Cr%	Fe%
SAE 2205	0.03	0.02	.20	0.03	1	2	3.5	6.5	23	Balance
AISI 304	0.06	-	-	0.07	0.9	1	0.2	8.4	16	Balance
AISI 308	0.045	0.03	-	0.08	1	2	-	10	19	Balance

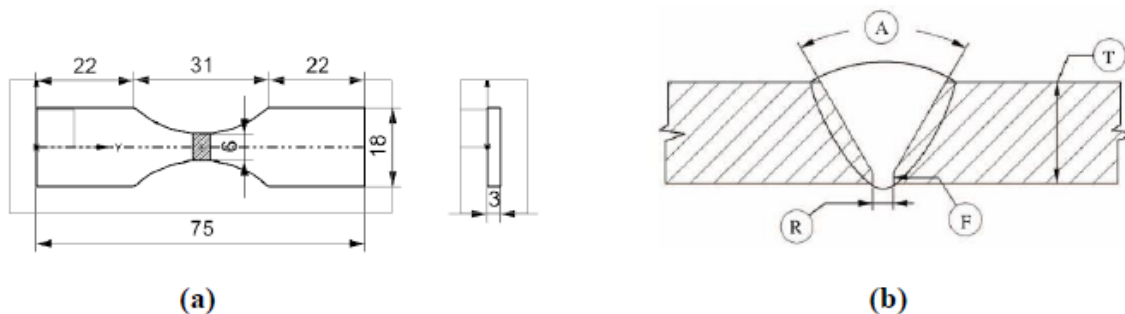


Figure 1: (a) Shows a tensile test specimen and (b) butt joint edge preparation method.

The 3D finite element model of the butt joint contains a total of 10 nodes, among these in the HAZ and in the fusion zone 4 nodes are present. The remaining nodes are present in the plate. Higher temperature and flux gradients are expected in and around the HAZ and fusion zone therefore, a relatively fine mesh is used within a distance of 5 mm from the weld centerline. Away from the HAZ the plate were divided into 2 regions of increasing element size as the distance from the weld centre line increases. Adaptive meshing was used throughout his study. For this purpose tetrahedral elements are used on both sides of the weld groove. The edge preparation details for the butt joint are shown in Figure 1 (b).

Table 2: Size of the butt joint

Thickness (T) in mm	Root gap (R) in mm	Groove angle (A) in deg.	Root face (F) in mm
6	2	45°	0

3. Results and Discussions

3.1. Optical Microscopy

The base metals DSS SAE 2205 and AISI 304 microstructures are shown in Figure 2 (a) and (b). In Figure 2 (a) elongated ferrite phase identified as yellow stripes are in a matrix of green austenite phase. The phase mixture is 60% ' γ ' and 40% ' δ ' ferrite which is rich with chromium. This observation is accordance with the observation made by Vigraman et al [9]. The average ' δ ' ferrite grain size is 6 μm and for the ' γ ' grains it is only 5 μm . At few places dark particles are seen, these particles are presumed to be ' σ ' phase. The microstructure shown in Figure 2 (b) is for the AISI 304 steel which reveals fine grains of austenite. The average grain size is 10 μm .

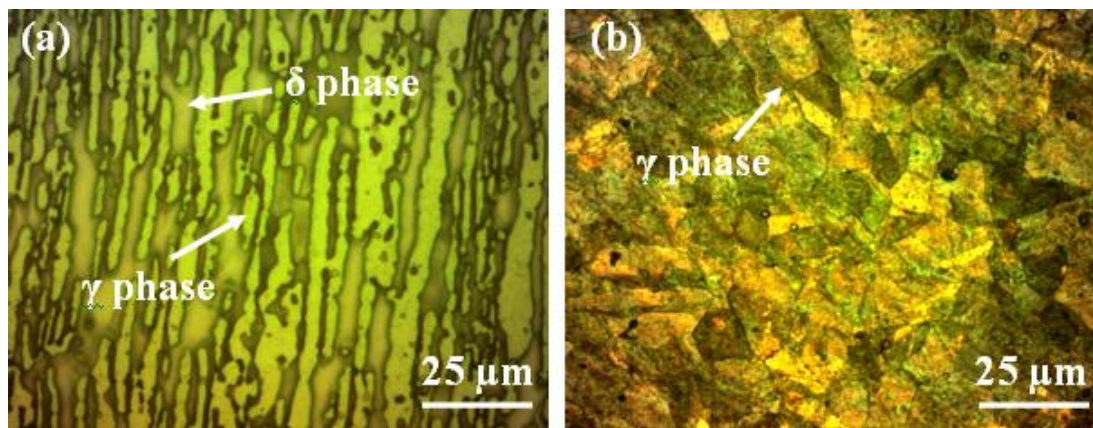


Figure 2: Base metal microstructures (a) for DSS SE 2205 and (b) AISI 304 steel.

In Figure 3 (a) heat affected zone (HAZ) is visible between the AISI 304 steel side and the weld metal AISI 308 stainless steel. The HAZ contains fine grains all along the fusion boundary. The grain size is only 2-3 μm . These fine grains are formed because of recrystallization at this zone. Away from the HAZ elongated grains are seen in the weld metal AISI 308 side. This weld metal has columnar grains and their growth is oriented towards the centre of the weld. The volume fraction of austenite phase is greater than the ferrite phase because the filler metal contains 10%Ni and 1.8%Mn. Further, adjacent to this ' γ ' phase ' δ ' ferrite phase is present. The presence of ' δ ' ferrite phase is attributed to increase in Chromium content in the weld metal. In the base metal AISI 304 side the region close to the HAZ very fine ' γ ' grains are noted and away from this zone coarse grains are seen. Even these grains are not so large and they are only 8-10 μm in size.

The microstructure shown in Figure 3 (b) is reveals the presence of columnar grains adjacent to the HAZ. These grains are elongated and arranged as alternate strips of ferrite and austenite. The thin strips are fragmented and appear to be fine grains. Along the ferrite grains lengthy dark phase is present which is identified as ' σ ' (sigma phase). This ternary phase is present at the grains of ' γ ' phase. The amount of ' σ ' phase is more and this phase formed because of segregation of iron, chromium and nickel at this region. The microstructure shown in Figure 3 (c) reveals the presence of a combination of fine and coarse grains in the weld metal. The weld metal during solidification solidifies as fine grains of γ and small amounts of δ ferrite. At several

places columnar grains emanating in the perpendicular direction to the joint and at the centre very fine grains are formed. The solidification rate is faster therefore, these grains are finer and have definite direction.

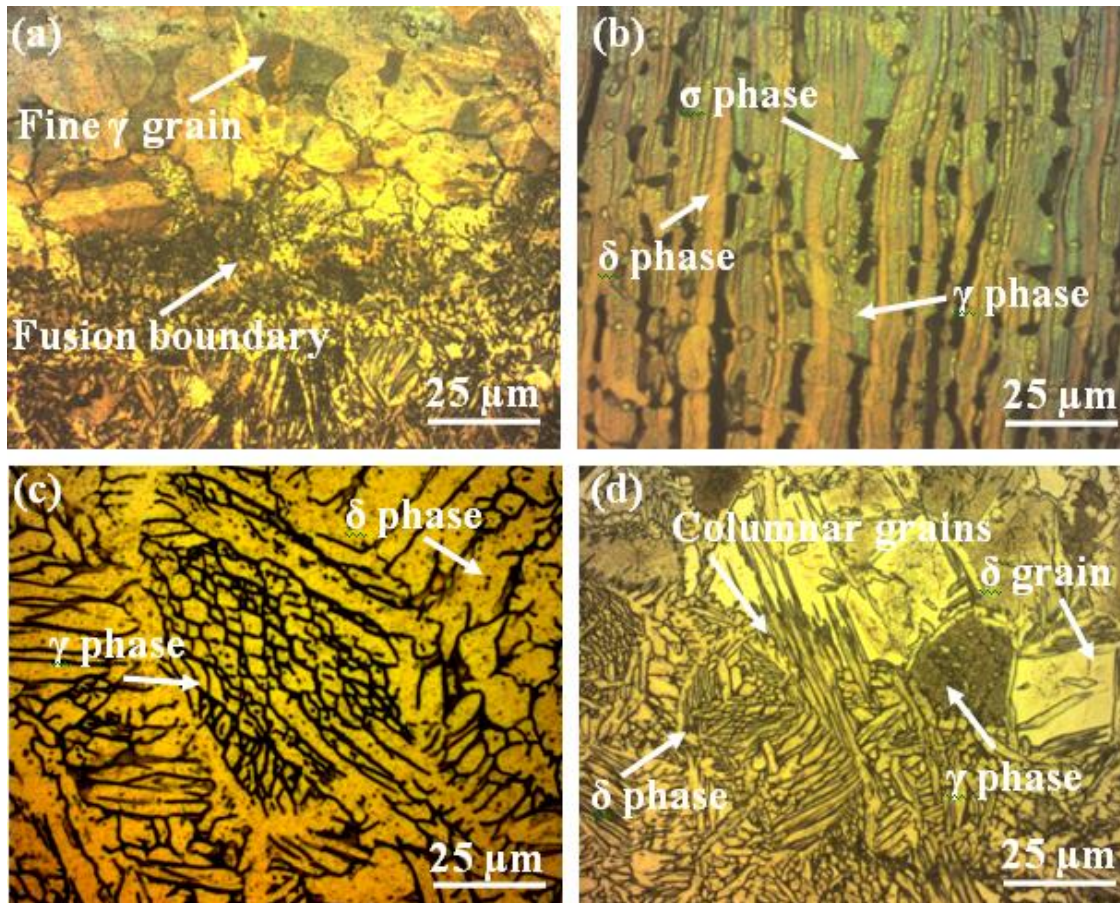


Figure 3: Optical microstructures for the welded joint processed at 110 Amp (a) heat affected zone between the AISI 304 and weld metal, (b) columnar grains adjacent to the HAZ, (C) weld metal and (d) weld metal and SAE 2205 interface.

A separable weld line is visible between the weld metal AISI 308 and the DSS SAE 2205 in the micrograph shown in Figure 3 (d). Close to the interface at the filler metal side few coarse grains are seen, these grains are identified as austenite and ferrite grains. Further, needle like growth is observed from the SAE2205 stainless steel side towards the filler metal side. These needles are identified as 'γ' phase formed during solidification of the weld metal. Adjacent to the interface in the SAE 2205 side columnar grains are seen and these grains are oriented in all directions. In the DSS side presence of columnar γ and δ phase is noted which indicates the HAZ. In the HAZ the columnar grains are finer and short in length to the one found in the base metal region. Therefore, recrystallization is the reason for the presence of these grains in this zone. A lengthy dark phase is noted away from the HAZ and in the base metal which is identified as 'σ' phase.

The micrograph shown in Figure 4 (a) shows a weld fused interface between the weld metal and the DSS SAE2205. Adjacent to this boundary in the weld metal austenite grains are seen. Also,

at few places long columnar grains are seen, these grains are identified as austenite grains. Further, at the austenite grain boundaries very fine recrystallized grains are noted. The micrograph presents a combination of fine and coarse austenite grains also, at few places very dark grains are noted which are formed because of etch defect. The amount of austenite phase is greater than the one seen in Figure 3 (d).

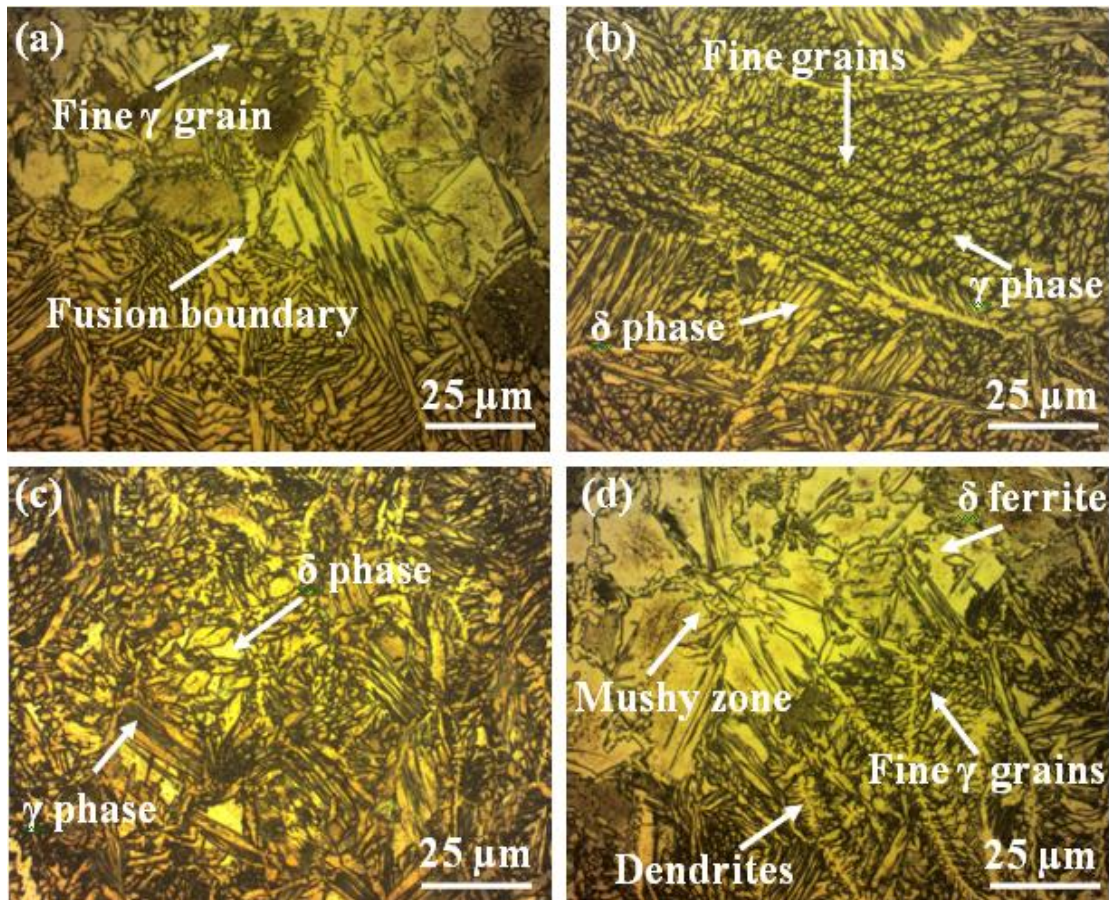


Figure 4: Optical microstructures for the welded joint processed at 130 Amp (a) heat affected zone between the AISI 304 and weld metal, (b) columnar grains adjacent to the HAZ, (C) weld metal and (d) weld metal and SAE 2205 interface.

Close to the interface at the filler metal side needle like growth is observed from the SAE 2205 stainless steel side towards the filler metal side. These needles are identified as ‘ γ ’ phase formed during solidification of the weld metal. Adjacent to the interface in the SAE 2205 side columnar grains are seen and these grains are oriented in all directions. In the DSS side presence of columnar γ and δ phase is noted which indicates the presence of HAZ. The columnar grains present in the HAZ are finer and short in length to the one found in the base metal region. The reason for this is attributed to recrystallization in this region. In the base metal SAE 2205 side ‘ σ ’ phase formation is not found for this joint welded at 130 Amp. In the HAZ very ultra fine grains of green in colour are seen and these grains are identified as γ grains as shown in Figure 4 (b). Adjacent to these ultra fine grains on both sides columnar grains are running parallel to these grains. They are less in number and presumed to be ‘ δ ’ ferrite. Perpendicular to these columnar

grains lengthly elongated thick grains are noted and these grains are primary ‘ γ ’ grains. The average grain size is very less and is only 2-3 μm .

The microstructure shown in Figure 4 (c) refers to the weld metal region of the joint obtained at 130 Amp. In the weld metal at few places very fine grains and throughout the matrix elongated grains are seen. The amount of ‘ δ ’ ferrite is around 20-30% and the remaining phase is ‘ γ ’ iron. At few places dark phase is present which is identified as ‘ σ ’ phase. A well distinguished heat affected zone (HAZ) is visible between the AISI 304 steel side and the weld metal AISI 308 stainless steel and is shown in Figure 4 (d). The HAZ contains fine grains all along the fusion boundary. The grain size is only 2-3 μm at the HAZ. These fine grains are formed because of recrystallization at this zone. Away from the HAZ elongated fine grains are seen in the weld metal AISI 308 side. This weld metal has columnar grains and their growth is oriented towards the centre of the weld. In the base metal AISI 304 side the region close to the HAZ very fine ‘ γ ’ grains are noted and away from this zone coarse grains are seen. Even these grains are not so large and they are only 10-12 μm in size.

3.2. Rockwell Hardness Test

A graphical plot between the measured points and the Rockwell values is shown in Figure 5. The hardness values were measured across the weld metal starting from one side of the base metal SAE 2205 to the other side of the base metal AISI 304 side passing through the weld metal AISI 308. The average hardness value at the base metal SAE 2205 side was Rc 36, on the weld metal it was Rc 27 and in the base metal AISI 304 the value was Rc 25 in Rockwell ‘C’ scale. At the recrystallized zone the average hardness value was Rc 32 at the SAE 2205 and AISI 308 side and at the AISI 308-AISI304 side, the hardness value was Rc 29. In the weld metal hardness values were decreasing because of dilution elements such as chromium, molybdenum and nickel from the weld metal towards the base metals. At the recrystallized zone fine grains were formed, these small grains increase hardness value up to Rc 32 and Rc 29.

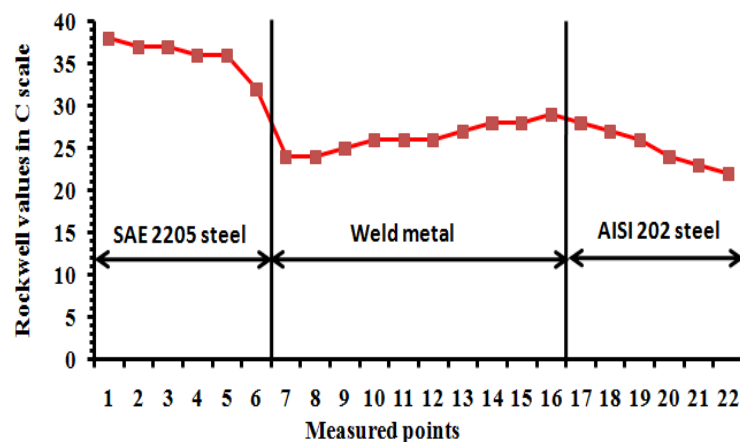


Figure 5: The Rockwell hardness values of the welded sample processed at 130 Amp.

The measured Rockwell hardness values were almost same for the welded samples processed at 110 and 120 Amp. Apurav Choubey et al [10] observed the hardness variation in the welded samples at various heat inputs at the base metal AISI 304 steel was not very high.

3.3. Tensile Test

The yield and tensile strength of the samples processed at 110 Amp were 314 and 527 MPa, respectively. For the samples welded at 120 Amp the yield and tensile strength were 325 and 542 MPa, respectively. The maximum yield and ultimate tensile strength of 354 and 549 MPa respectively, was obtained for the sample processed at 130 Amp. The fracture took place at the base metal AISI304 side and the mode of fracture is ductile in nature. The weld joints exhibited a joint efficiency of 102 % in comparison with the base metal AISI304 steel. But the joint efficiency was only 83% in comparison with the tensile strength of 660 MPa for the base metal SAE 2205. The reason for decrease in tensile strength was attributed to the filler metal which possessed a tensile strength of 540 MPa.

The tensile strength values were low for the welded joints obtained at 110 in comparison with the samples welded at 130 Amp. The difference in yield and tensile strength between the joints obtained at 120 Amp and 130 Amp was 8.9% and 2%, respectively. On the other hand the ductility was 37% for the samples produced at 110 Amp. The ductility was 32% for the samples welded at 120 Amp. The ductility was 33% for the samples welded at 130 Amp. The reason for decrease in ductility of the samples welded at 120 and 130 Amp was attributed to grain coarsening in the base metal AISI 304 steel. Pascual et al [11] obtained a tensile strength of 501 MPa for the joints made between the AISI 316 steel using AISI 308 steel as filler material. In the current study the tensile strength obtained for all the three current values are greater than the values reported by Pascual et al [11]. Wichan Chuaiphon et al [12] explained the variation in tensile strength was due to absorption interstitial elements in the joint region.

The stress strain diagrams for the samples processed at 110 and 130 Amp are shown in Figure 6. In all the tensile test specimens fracture took place in the base metal AISI304 steel side and the mode of fracture was ductile in nature. This in accordance with the published work by Subodh Kumar et al [13]. The fracture site was fibrous in nature which indicated the mode of fracture was ductile. Further, the ductility values obtained for the tensile test samples corroborated the mode of fracture was ductile. There was no cleavage fracture and river pattern was not formed at the fractured surface, therefore, the mode of fracture was ductile.

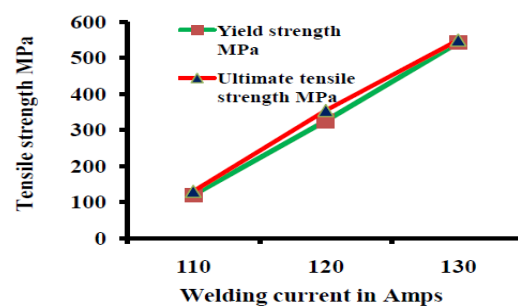


Figure 6: The tensile strength of the welded joints.

3.4. Combined Thermal and Stress Analysis

The temperature distribution of the welded butt joint of each node is shown Fig 7 (a)- (f). The temperature profile indicates that at the centerline of the weld it is maximum and as the distance

increases away from the centerline it decreases. The maximum temperature is 1400 °K and the minimum temperature in the plate region is 300 °K. The peak temperature in the joint is at least between 1300 and 1400 °K which conform to the analysis done by Justin D. Francis.. The temperature may reach higher values at certain nodal points, as would be expected in a practical welding situation. At the centre of the weld temperature increases when the welding time increases.

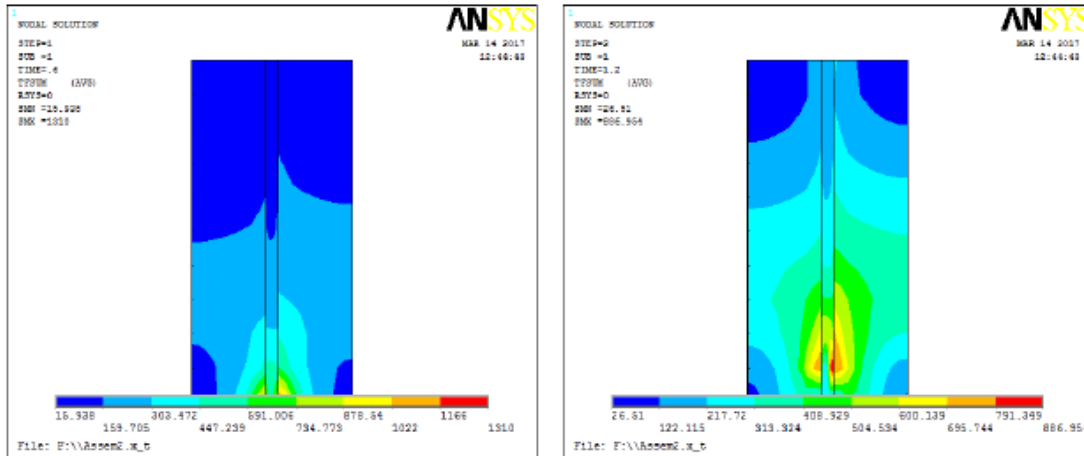


Figure 7: (a) Moving heat source at node 1 and (b) Moving heat source at node 2

In the beginning of welding the heat source is at the edge of the plate, therefore, the maximum temperature is not very high at the weld centre line as seen in the Fig 7 (a). As the heat source moves, at the centre of the weld line the maximum temperature is indicated by red color in the ANSYS output graphs shown in Fig7 (b)-(f). Along the Y-axis maximum temperature is observed at the SAE 2205 side, this indicates the maximum heat transfer is in the transverse direction to the axis of the heat source. The difference in temperature between ANSYS and experimental value is less than 10%. Justin D. Francis [14] observations are conforming to the output obtained by these authors. The residual stress is built in the joint region because welding is carried out in highly restrained condition. A maximum of 85 MPa was obtained as residual stress for the joints made between dissimilar stainless steel grades SAE 2205 and AISI 304.

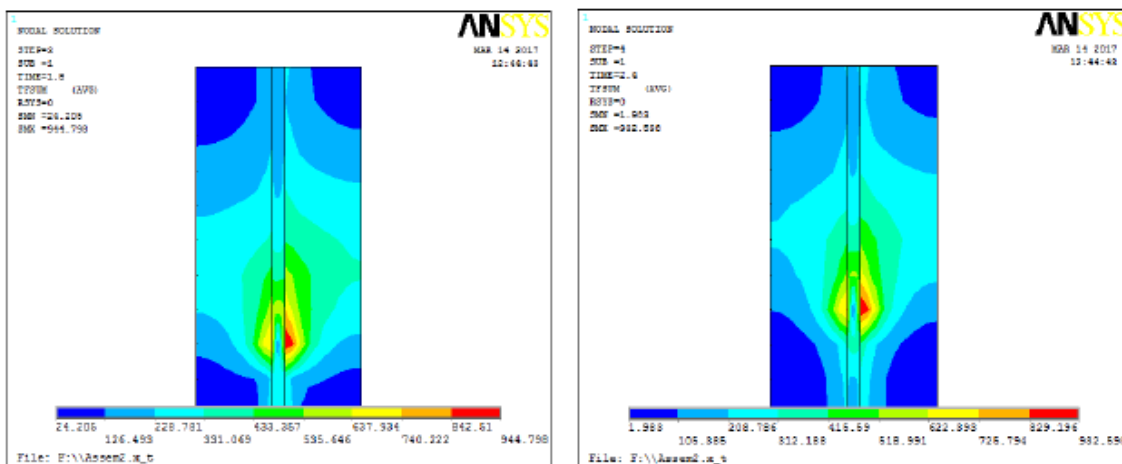


Figure 7: (c) Moving heat source at node 3 and (d) Moving heat source at node 4

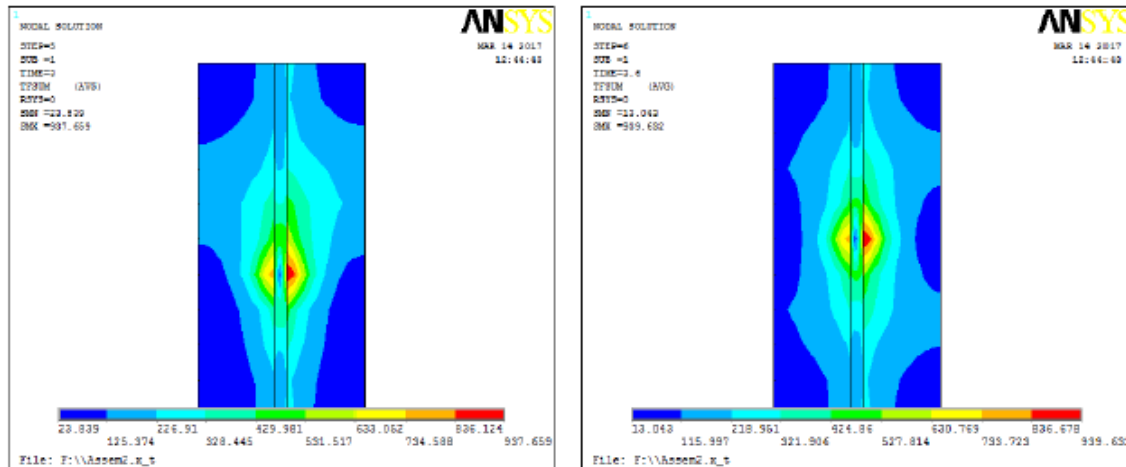


Figure 7: (e) Moving heat source at node 5 and (f) Moving heat source at node 6

4. Conclusions

- TIG welding was performed with SAE 2205 with AISI304 steel with AISI308 austenitic stainless steel filler material.
- The maximum tensile strength of 549 MPa was obtained for the samples processed at 130 Amp. Heat input variation was having an effect on tensile strength of the joints.
- The hardness values were on the higher side at the base metal SAE 2205 than the weld metal AISI308 and base metal AISI 304 steel. A maximum hardness value of Rc 36 was observed at the base metal SAE 2205 side for the sample welded at 130 Amp. The increase in hardness values were attributed to presence of more amounts of chromium and σ phase in the base metal SAE 2205.
- Ultra fine grains and fine grains were formed at the HAZ zone in all the samples.
- A maximum Von Mises stress of 85 MPa is obtained for the weld joints made between stainless steel AISI 304 and stainless steel SAE 2205.

References

- [1] Kohyama A, Kohno Y, Baba K, Katoh Y and Hishinuma A, Microstructural changes in welded joints of 316 SS by dual-ion irradiation, *Journal of Nuclear Materials*, 1992, 191-194;722-727.
- [2] Juang S.C and Tarng Y.S, Process parameter selection for optimizing the weld pool geometry in the tungsten inert gas welding of stainless steel. *Journal of Materials Processing Technology* 122 (2002), P 33–37.
- [3] Kang B.Y, Yarlagadda K.D.V. Prasad, Kang M.J, Kim H.J and Kim I.S, The effect of alternate supply of shielding gases in austenite stainless steel GTA welding, *Journal of Materials Processing Technology*, 209, 2009, pp-4722–4727.
- [4] Raghuvir Singh, Suri N.M, and Jagjit Randhawa Optimization of Process Parameters for TIG welding of 304L Stainless Steel using Response Surface Methodology. *International Journal of Mechanical Science and Civil Engineering* Volume 2 Issue 2 (June 2013 Issue), P 36-40.
- [5] Ahmet Durgutlu, Experimental investigation of the effect of hydrogen in argon as a shielding gas on TIG welding of austenitic stainless steel, *Materials and Design*, 25, 2004, pp- 19–23.

- [6] Zuheir Barsoum “Residual stress analysis and fatigue assessment of welded steel structures” is presented for public review and doctoral examination on April 25th 2008 at 10.00 in E1,KTH, Lindstedtsvägen 3, Stockholm.
- [7] Janakiram.G.,Vijay.S, Dr.M.Venkateswara Rao“Analysis Of Temperature Distribution Of Different Welded Joints In Ship Building”Vol. 1 Issue 6, August – 2012.
- [8] Ya Tao Wu “Residual Stress Study at the Dissimilar Metal Butt Joint due to the Weld Overlay Repair on a Nuclear Power Plant Nozzle Using ANSYS “Rensselaer Polytechnic Institute Hartford, CT April, 2012.
- [9] Vigraman T, Narayanasamy R and Ravindran D, “Microstructure and mechanical property evaluation of diffusion-bonded joints made between SAE 2205 steel and AISI 1035 steel” Materials & Design, Volume 35, March 2012, Pages 156–169.
- [10] Apurv Choubey, Vijaykumar S. Jatti, Influence of heat input on mechanical properties and microstructure of austenitic 202 grade stainless steel weldments, Wseas Transactions on Applied and Theoretical Mechanics, Volume 9, 2014, Pages 222-228.
- [11] Pascual M, Salas F, Carcel F. J, Perales M and Sánchez A, TIG AISI-316 welds using an inert gas welding chamber and different filler metals: Changes in mechanical properties and Microstructure, REVISTA DE METALURGIA, Vol. 46 (6), 2010pages 493-498,.
- [12] Wichan Chuaiphon, Loeshpahn Srijaroenpramong. Materials Processing Technology 214 (2014) 402– 408.
- [13] Subodh Kumar and Shahi A.S.,Materials & Design, 32 (2011) 3617–3623.
- [14] Justin D. Francis“Welding Simulations of Aluminium Alloy Joints by Finite ElementAnalysis” Blacksburg, Virginia, April 2002.

*Corresponding author.

E-mail address: tmvig.yanka@ gmail.com